Neuron, Volume 64

Supplemental Data

Extracellular Engrailed participates in the topographic guidance of retinal axons in vivo

Andrea Wizenmann[*], Isabelle Brunet[*], Joyce S. Y. Lam[*], Laure Sonnier[*], Marine Beurdeley, Konstantinos Zarbalis, Daniela Weisenhorn-Vogt, Christine Weinl, Asha Dwivedy, Alain Joliot, Wolfgang Wurst[+], Christine Holt[+], and Alain Prochiantz[+]

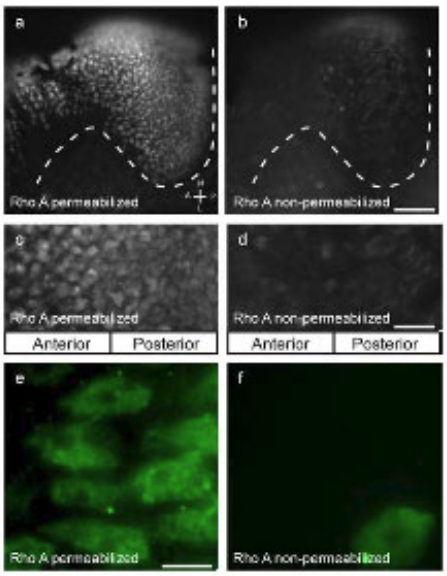

Figure S1: RhoA immunostaining is uniform in permeabilised tectum and absent without permeabilisation

Intracellular RhoA immunostaining is negligible without tissue permeabilization.

(a-b) Dorsal view of stage 37/38 flat-mounted Xenopus tecta showing RhoA immunostaining in permeablized (a) and non-permeablized (b) conditions. White dashed lines demarcate tectal borders. Higher magnification views are shown below in (c-f). (e) Immunostaining is characteristically cytoplasmic in permeabilised tectal cells and rarely occurs without permeabilization (f). M, medial ; L, lateral; A, anterior; P, posterior. Scale bars: (a-b) 100μm, (c,d) 30μm (e-f) 10μm.

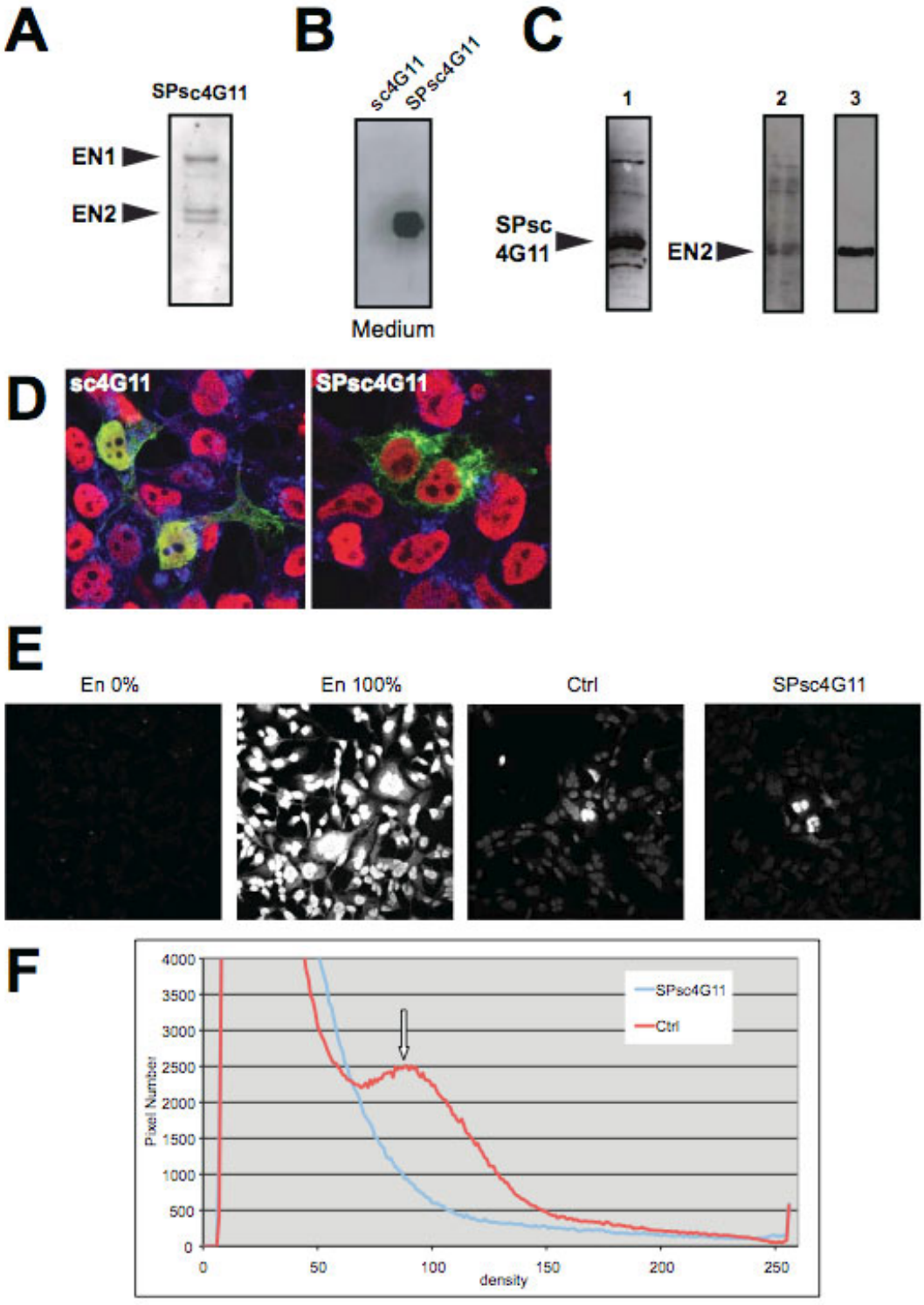
A
SPsc4G11
EN1
EN2
B
sc4G11
SPsc4G11
Medium
C
1
2
3
SPsc
4G11
EN2
D
sc4G11
SPsc4G11
E
En 0%
En 100%
Ctrl
SPsc4G11
F
Pixel Number
density
SPsc4G11
Ctrl
4000
3500
3000
2500
2000
1500
1000
500
0
0
50
100
150
200
250

Figure S2: functional characterization and validation of anti-En1/2 single chain antibodies

(**A**) The HEK:S4G11 cell line expressing the secreted form of the single chain anti-En1/2 antibody (SPsc4G11) was cultured for 48h on T75cm2 flask in complete medium supplemented with doxycycline (1µg/ml) to induce antibody expression. The supernatant containing SPsc4G11 was used as a source of antibody to detect purified En1 and En2 by Western blotting (1µg per slot) with the ECL+ Amersham revelation kit. En2 runs as a doublet. Since the single chain antibodies does not contain an Fc domain, its presence was revealed with the 9E10 anti-myc antibody thanks to the myc tag introduced in the sequence (see material and methods). This demonstrates that the single chain antibody recognizes En1 and En2.

(**B**) Secretion of En1/2 single chain antibody (SPsc4G11)

Conditioned media from a 1 day culture of HEK293 clones stably expressing a secreted (Spsc4G11), or non secreted (sc4G11) single chain antibody against En1/2 were prepared as described in A, and purified on a Nickel purification column (Hitrap) thanks to a poly-Histidine (His6) stretch present in the sequence of the antibody. The eluted material was separated on SDS PAGE and the presence of the single chain antibodies was revealed by western blot with 9E10 anti-myc antibody.

(**C**) The myc-tagged secreted single chain antibody against Engrailed (SPsc4G11) electroporated (2µg/ml) into E2 chick tectum is expressed at E3 (anti-myc lane 1, western blot) and immunoprecipitates endogenous Engrailed (lane 2). Lane 3 corresponds to purified Chick En2.

(**D**) Intracellular localization of Spsc4G11 and sc4G11

HEK293 clones stably expressing En2 were transiently transfected with a plasmid encoding a secreted (SPsc4G11) or non secreted (sc4G11) single chain antibody. One day after transfection, cells were fixed and immunostained for En2 (anti-En, red) and single chain antibodies (green, 9E10). Note the contrasted distribution of the two antibodies, in particular the absence of SPsc4G11 in the nucleus.

(**E**) Inhibition of En2 inter-cellular transfer by SPsc4G11 single chain antibody

En2 Expressing HEK293 were either culture alone (En 100%) or co-cultured (at a 1:10 ratio) with naïve HEK293 cells (Ctrl) or HEK293 clone stably expressing SPsc4G11 (control HEK alone are shown in En 0%). Two days after, cells were fixed and immunostained with 86.8 anti En1/2 antibody. Note that SPsc4G11 blocks En2 intercellular spreading.

(**F**) For the two co-culture conditions (Ctrl or SPsc4G11), seven fields (375 μm^2) were randomly selected and analyzed by confocal microscopy. For each condition, the values of the density histograms (0: Background) of the seven fields were pooled and plotted. Inter-cellular transfer of En2 was characterized by the presence of a peak of low intensity over the background (arrow), which was absent in SPsc4G11 co-cultures.

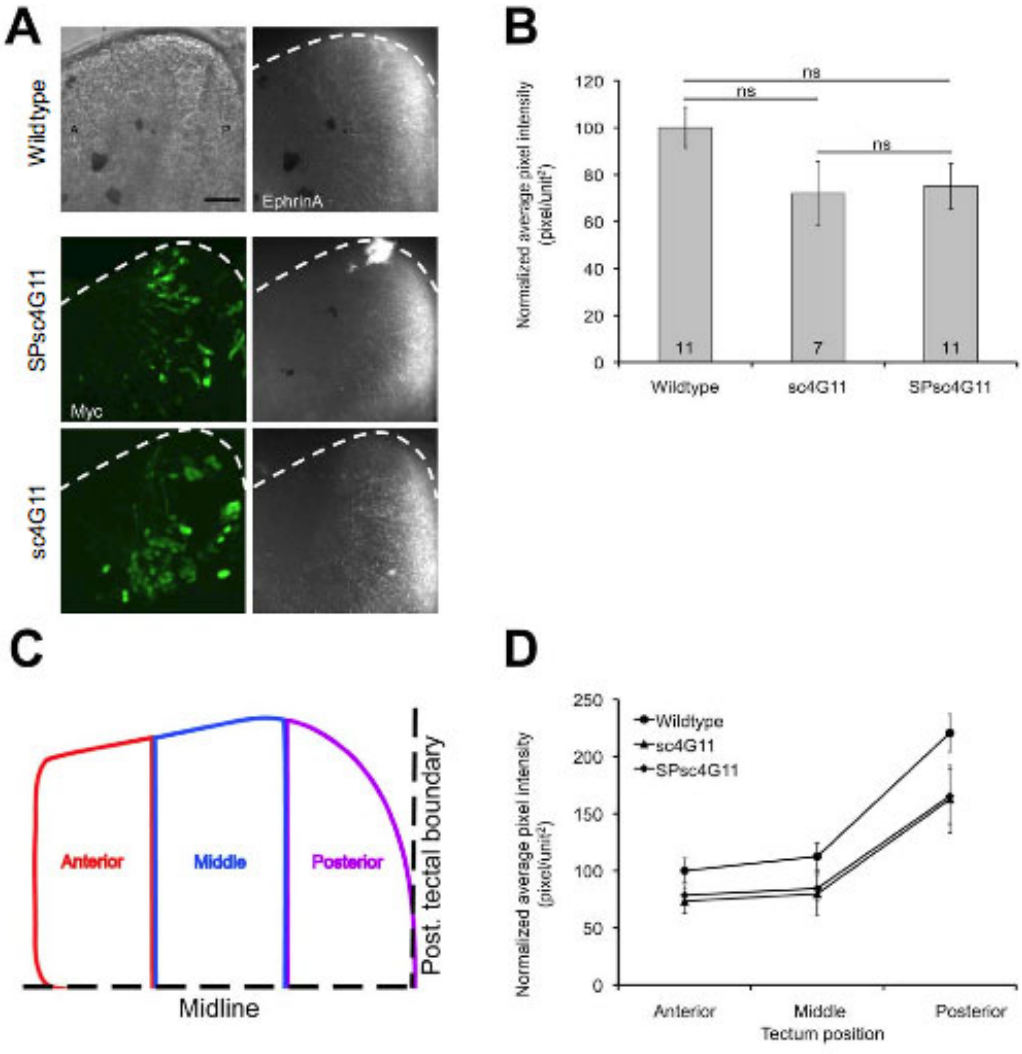
A
Wildtype
A
P
EphrinA
SPsc4G11
Myc
sc4G11
B
Normalized average pixel intensity (pixel/unit²)
ns
ns
ns
120
100
80
60
40
20
0
11
7
11
Wildtype
sc4G11
SPsc4G11
C
Anterior
Middle
Posterior
Post. tectal boundary
Midline
D
Normalized average pixel intensity (pixel/unit²)
Wildtype
sc4G11
SPsc4G11
250
200
150
100
50
0
Anterior
Middle
Posterior
Tectum position

Figure S3: Expression of extracellular Engrailed antibody does not modify EphrinA gradient in the tectum

(**A**) Images showing extracellular EphrinA distribution in stage 43/44 Xenopus tecta. EphrinA is bound to recombinant mouse EphA3/human Fc chimera under non-permeabilzed conditions and visualized by immunostaining to the Fc tag. Cells expressing single chain anti-Engrailed antibodies (secreted or not), identified by myc immunostaining, are abundant in the tectum. EphrinA antero-posterior gradient is not disrupted in tecta expressing secreted (SPsc4G11) or non-secreted (sc4G11) anti-Engrailed and is comparable to wild type tecta. This, in addition precludes that the secreted antibody may have an activity associated with its diffusion in contralateral territories. White dashed line denotes the lateral boundary of the tectum. A, anterior; P, posterior. Scale bar: 50μm.

(**B**) Bar graph showing the normalized average pixel intensity of extracellular EphrinA staining in the whole tectum. Average pixel intensities have been normalized to that of the wild type. Fluorescent signal intensity of extracellular EphrinA staining in tecta expressing secreted (SPsc4G11) or non-secreted anti-Engrailed (sc4G11) is not significantly different from wild type tecta (Kruskal-Wallis test). Numbers in the bars denote the number of tecta analyzed.

(**C**) Diagram illustrating the division of the tectum into thirds along the anterior-posterior axis (anterior, middle and posterior). The average pixel intensity of extracellular EphrinA immunofluorescence signal was measured for each tectal third.

(**D**) Comparison of the normalized pixel intensity values of the anterior, middle and posterior tectal thirds shows that the EphrinA antero-posterior gradient is not disrupted in SPsc4G11 or sc4G11-expressing tecta. Pixel intensities were normalized to the wild type anterior tectum, and are not significantly different between groups (Kruskal-Wallis test). Data are presented as mean ± SEM.

Error bars indicate standard deviation.

A

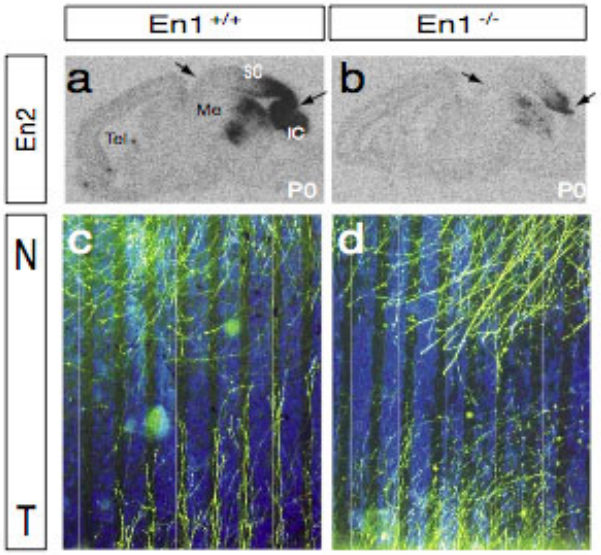

B

		0	1	2	n
EN1 $^{-/-}$	T	30	-	-	30
	N	30	-	-	30
EN1 $^{+/+}$	T	-	4	36	40
	N	41	-	-	41

C

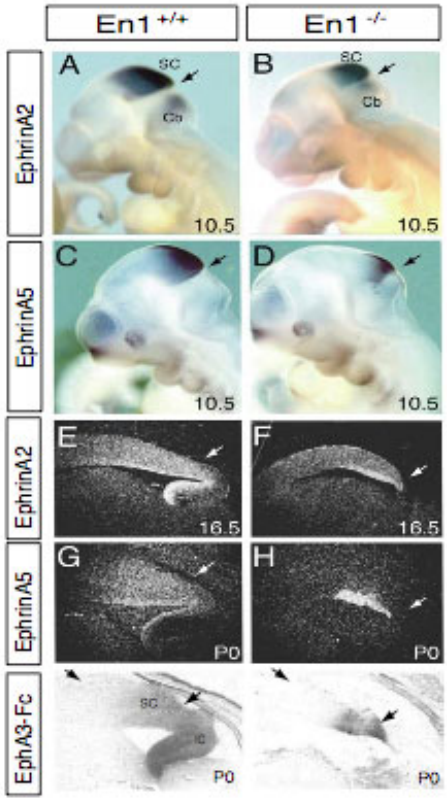

Figure S4: Posterior SC membranes from En1 mutants fail to repel temporal axons

(A) At birth (P0), En2 mRNA (arrows) is strongly expressed in the Inferior Colliculus (IC) and in a graded manner in the SC in WT (SC indicated by arrows in A). In the En1 mutant ($En1^{-/-}$), IC is almost missing and En2 expression in SC is strongly reduced. Also note that SC is reduced in size.

In a stripe assay with membranes from wild type ($En1^{+/+}$) mice, temporal (T) axons (green fluorescence) are repelled by membranes from posterior SC (indicated by blue lines), whereas, nasal axons grow out randomly. This preference of temporal axons for anterior SC membranes is abolished when the SC membranes are derived from En1-/- knockouts.

(B) A scoring system (2 for maximal repulsion and 0 for no repulsion of axons) showed that temporal axons are not repelled by posterior membranes that are derived from $En^{-/-}$ SC.

(C) From E10.5 to birth, EphrinAs mRNAs and proteins (revealed by EphA3-Fc fusion proteins) are strongly expressed in the IC and in a posterior high anterior low gradient in the SC in heterozygote animals. In the $En1^{-/-}$ mutant EphrinAs SC expression is reduced but maintained. The arrows indicate the extension of the SC.

A

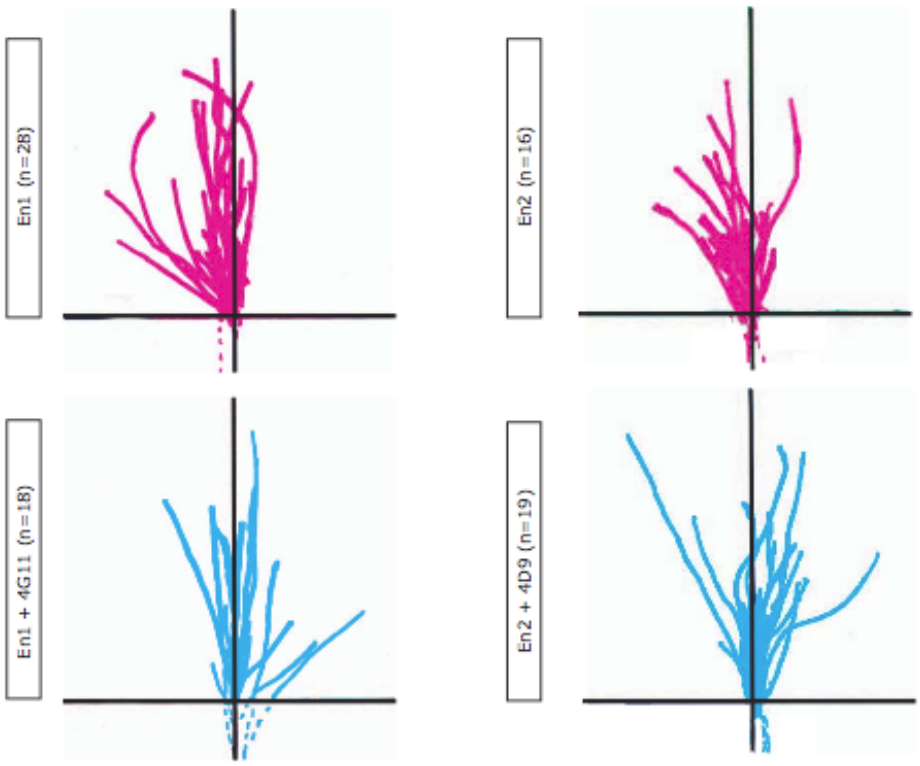
En1 (n=28)
En2 (n=16)
En1 + 4G11 (n=18)
En2 + 4D9 (n=19)

B

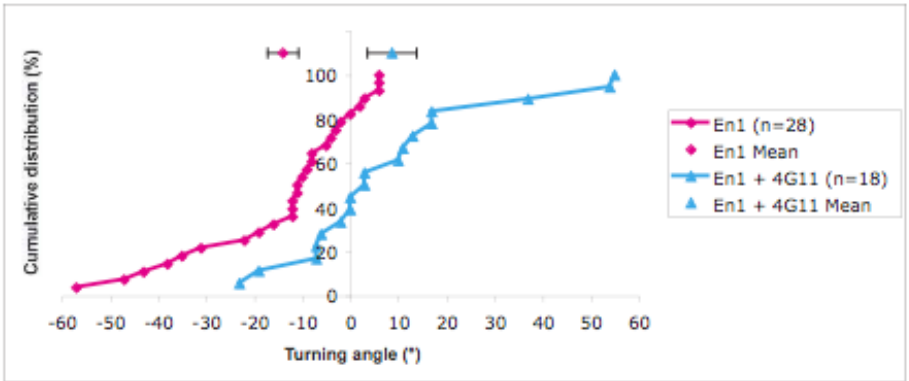
Cumulative distribution (%)
100
80
60
40
20
0
-60 -50 -40 -30 -20 -10 0 10 20 30 40 50 60
Turning angle (°)
En1 (n=28)
En1 Mean
En1 + 4G11 (n=18)
En1 + 4G11 Mean

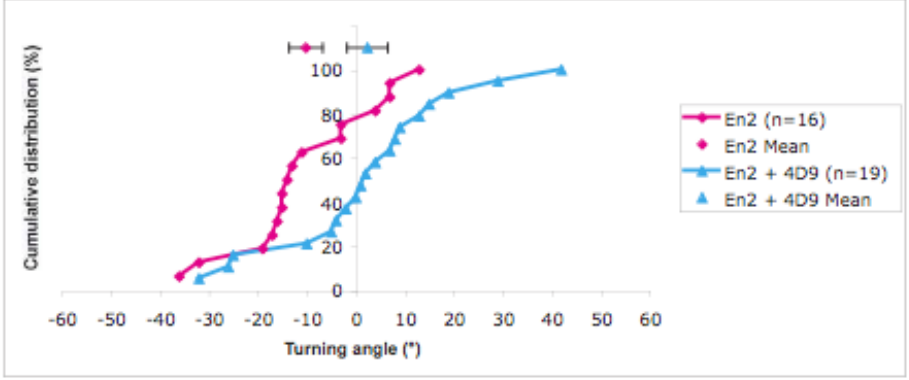
Cumulative distribution (%)
100
80
60
40
20
0
-60 -50 -40 -30 -20 -10 0 10 20 30 40 50 60
Turning angle (°)
En2 (n=16)
En2 Mean
En2 + 4D9 (n=19)
En2 + 4D9 Mean

Figure S5: En2 and En1 both repel temporal axons *in vitro*

(A) The trajectory plots show traces depicting the trajectory of axon extension during the 1-hour turning assay. Dotted lines below the x-axis indicate the shift in the position of axons after the 1 hour assay. The gradient was created by pulsatile application with a micropipette positioned on the top right corner. In addition, we have verified that En1 attracts nasal axons *in vitro*. En1 triggered attraction (+13° ± 5.6°) was abolished (p= 0.04 using Kolmogorov-Smirnov test, p= 0.0336 using Mann-Whitney test) when the protein was incubated with the blocking antibody 4G11 (-3.7° ± 5.4°).

(B) The top panel shows the cumulative distribution of angles measured on Temporal axons exposed to a gradient of either En1 (red line) or En1 pre-incubated with a specific neutralizing antibody (4G11, blue line). En1 triggered repulsion (-14° ± 3.1°) was abolished (p= 0.002 using Kolmogorov-Smirnov test, p= 0.0005 using Mann-Whitney test) when the protein was incubated with the blocking antibody 4G11 (8.7° ± 5.1°). The bottom panel shows the same results with En2 (-10.2° ± 3.4°) and the neutralizing 4D9 antibody (2.4° ± 4.2°). (p= 0.04518 using Kolmogorov-Smirnov test, p= 0.02651 using Mann-Whitney test).

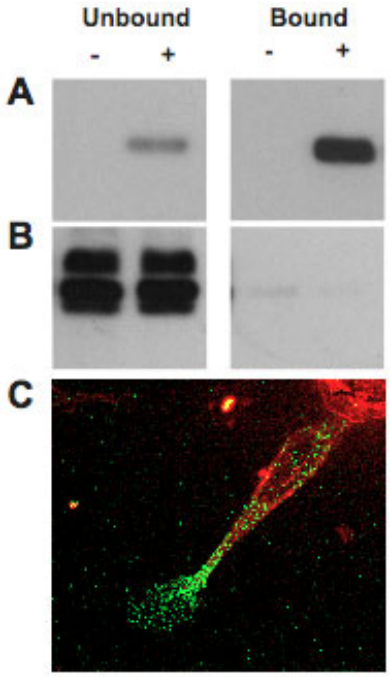
Unbound
Bound
-
+
-
+
A
B
C

Figure S6: Absence of interaction between Engrailed and EphrinA5

HEK293 cells were transfected with HA-Tagged EphrinA5 alone (-) or co-transfected with EphrinA5 and Engrailed-2 tagged with 6 histidines (+) allowing direct attachment to Nickel columns. Extracts were loaded on Nickel columns to trap Engrailed-2 and bound and unbound fractions were tested for the presence of Engrailed-2 (A) and EphrinA5 (B).

Most Engrailed-2 was bound on the Nickel column but no EphrinA5 was retained with the transcription factor demonstrating the absence of direct interactions between the two molecular entities.

In C, is shown a HEK293 cells co-expressing Engrailed-2 (green) and EphrinA5 (red) in absence of permeabilization (extra-cellular proteins). Note the high extra-cellular expression and the absence of co-localization of the two proteins.

Supplementary Materials and Methods:

Immunohistochemistry in Xenopus optic tectum

Xenopus stage 37/38 embryos were anaesthetized in 0.4g/L MS222 (3-aminobenzoic acid ethyl ester methanesulphonate salt, Sigma). Surgical procedures were performed to expose the tectum as described (Chien et. al., 1993, Strochlic et al., 2008). Embryos were fixed for 10 minutes in 4% paraformaldehyde at room temperature, washed 3 times for 5 minutes in PBS and permeabilized for 30mins in 0.5% TritonX-100 (Sigma) in PBS then incubated overnight in primary antibodies (Rho-A, SC-179, Santa Cruz Biotechnology, diluted 1:1000) in PBS containing 5% goat serum. The next day embryos were washed 3 times for 5 minutes in PBS, blocked for 1 hour in PBS containing 5% goat serum and incubated for 2 hours with Goat anti Rabbit Alexa 488 secondary antibody (diluted 1: 750, Invitrogen) at room temperature. Samples were washed 3 times for 10 minutes in PBS and re-fixed for 30 minutes in 4% paraformaldehyde at room temperature. After 3 washes for 5 minutes in PBS, samples were incubated for 5 minutes with 4'-6- Diamidino-2-Phenylindole (DAPI, diluted 1:10000, Sigma) in PBS, followed by 3X 5 minute washes in PBS. Brains were subsequently dissected out in PBS and mounted in FluoroSave ™ (Calbiochem) as described (Strochlic et al., 2008). Mounted brains were visualized under Nikon fluorescence microscope using 10x (Nikon Plan Apo, 0.45), 20x (Nikon Plan Apo, 0.75) and 100x (Nikon Plan Apo, 1.40 oil) objectives. Images were captured by Orca-ER Hamamatsu CCD camera using Openlab 4.0.2 software (Improvision).

$En1^{-/-}$ knockout mice

The $En1^{-/-}$ mice are kept on a heterogeneous genetic background (C57BL/6J//SV129). Homozygous En1 mutants were chosen after their defect in forelimb development and confirmed with southern blot analysis.

Xenopus retinal explant culture and growth cone turning assay

Embryos were obtained by in vitro fertilization of oocytes from Xenopus laevis stimulated with human chorionic gonadotropin (Sigma). Embryos were raised in 0.1X Modified Barth Saline (MBS) at pH 7.4, and staged according to Nieuwkoop and Faber (Nieuwkoop and Faber, 1967). The extreme temporal third of stage 32-33/34 retinas were explanted onto 50 mm glass-bottomed

Petri dishes (Matek) pre-coated with 10μg/mL poly-L-lysine and 5 or 10μg/mL laminin (Sigma). Cultures were grown at 20°C for 12-26 hours in 60% L15 (Gibco, Life Technologies) and 0.1% penicillin/streptomycin/fungizone (Gibco, Life Technologies) pH 7.6.

Stable gradients of Engrailed1/2 (10 to 20 μg/ml) protein were formed as described previously (Lohof et al., 1992) by pulsative ejection of Engrailed or Engrailed protein incubated with monoclonal antibody (4G11 antibody against mouse Engrailed 1, 4D9 antibody against chicken Engrailed 2, 1:10, 30min) using a Picospritzer (General Valve). The micropipette was positioned 100μm away from the center of an isolated growth cone, at 45° to its direction of growth, and digital images were captured using a Quantix camera (Photometrics) at 0 and 60 minutes. Under well-established conditions, stable concentration gradients of 5%-10% per 10μm are established; the concentration of protein reaching the growth cone is approximately 10^{-3} lower than in the pipette (Lohof et al., 1992). The turning angle was defined by the angle between the original direction of neurite extension and a straight line connecting the positions of the growth cone at the onset and the end of the turning assay. Only axons that had extended more than 10 μm during 60 minutes were analyzed. Data are presented as cumulative distribution and trajectory plots. Statistical significance was analyzed by the Kolmogorov-Smirnov test and by the Mann-Whitney test.

Supplemental References

Lohof, A.M., Quillan, M., Dan, Y., and Poo, M.M. (1992). Asymmetric modulation of cytosolic cAMP activity induces growth cone turning. J. Neurosci. 12, 1253–1261.

Nieuwkoop, P., and Faber, J. (1967). Normal table of Xenopus laevis (Daudin), 2nd edition (Amsterdam: North-Holland Publishing Company)